

Lattice BGK simulations of macrodispersion in heterogeneous porous media

L. Talon, J. Martin, N. Rakotomalala, and D. Salin

Laboratoire FAST, UMR 7608, CNRS et Universit es Paris 6 et 11, Campus d'Orsay, Orsay, France

Y. C. Yortsos

Department of Chemical Engineering, University of Southern California, Los Angeles, California, USA

Received 22 April 2002; revised 6 August 2002; accepted 13 November 2002; published 22 May 2003.

[1] We use the extended Darcy's law, which also accounts for the Brinkman correction, to study macrodispersion in a two-dimensional (2-D) porous medium. The former is necessary when permeability changes fast at a relatively small scale, and in general, it is a more complete description of flow in a heterogeneous medium. Lattice-gas methods are ideally suited to simulate such flows. Simulations using a lattice BGK method and a small-fluctuation approach are described for an isotropic, exponentially decaying correlation function of the permeability field. The analytical results contain the additional parameter K_l/λ^2 (where K_l and λ are the typical permeability and velocity variation length, respectively), the sensitivity to which was studied. As expected, the contribution of the Brinkman effect is insignificant for typical field values of this parameter, in which case, the classical results are recovered. At larger values, for example, for heterogeneous media of a small correlation length, and possibly in laboratory applications, the Brinkman correction leads to a decrease in macrodispersivity, reflecting the smoothing effect of the Brinkman correction on the velocity field. Nonetheless, for practical values of the parameters, this reduction is no larger than 50% of the classical expression. The small fluctuation theory was found to be in good agreement with the simulations, provided that it was consistently applied (namely, by not mixing first-order with second-order expansions). The results also show that lattice-gas simulations can be usefully employed to study macrodispersion in heterogeneous porous media. **INDEX TERMS:** 1829 Hydrology: Groundwater hydrology; 1869 Hydrology: Stochastic processes; 1832 Hydrology: Groundwater transport; 5114 Physical Properties of Rocks: Permeability and porosity; 5139 Physical Properties of Rocks: Transport properties; **KEYWORDS:** groundwater hydrology, groundwater transport, stochastic processes, transport properties

Citation: Talon, L., J. Martin, N. Rakotomalala, D. Salin, and Y. C. Yortsos, Lattice BGK simulations of macrodispersion in heterogeneous porous media, *Water Resour. Res.*, 39(5), 1135, doi:10.1029/2002WR001392, 2003.

1. Introduction

[2] Permeability heterogeneity in porous media is a well-recognized factor in many practical applications, in fields such as hydrology, petroleum and environmental engineering. Heterogeneities create preferential flow channels, which greatly enhance the spreading of pollutants, or, conversely lead to the bypassing of targeted zones containing organic liquids (such as oil or NAPLs, in the respective applications of oil recovery or aquifer remediation). The influence of heterogeneity on the field-scale dispersion of passive tracers has been studied extensively. Stochastic continuum approaches [Dagan, 1982; Gelhar and Axness, 1983; Dagan, 1984, 1989; Rubin, 1990; Hsu, 1999, 2000], based on Darcy's law and the advection-dispersion equation, have provided a significant understanding of the macroscale dispersion as a function of the statistical properties of the permeability field. These theories have compared favorably to conventional numerical simulations [Ababou et

al., 1989; Bellin et al., 1992; Jussel et al., 1994; Tompson and Gelhar, 1990; Chin, 1997].

[3] When the permeability fluctuation is over small distances, Darcy's law may not adequately describe the conservation of momentum. It is well known that Darcy's law breaks down near discontinuities in permeability (for example, across different permeability blocks or at the free liquid-porous medium interface). To connect the resulting discontinuities, an additional macroscale viscous term (the Brinkman correction [Brinkman, 1947]) is routinely added to Darcy's equation, leading to

$$\vec{\nabla}P = -\frac{\mu}{K}\vec{V} + \mu_e\Delta\vec{V} \quad (1)$$

where μ_e is an effective viscosity. The Stokes-type term above allows for a continuous solution of the velocity field for arbitrary permeability fields. Even though (1) has not been rigorously derived for arbitrary permeability distributions, it contains the correct phenomenological terms and it is more complete than Darcy's law in the case of arbitrary heterogeneity (see also below). The lattice Boltzmann simulator to be described here naturally accounts for these terms and could

be used as a more complete model for the numerical simulation of such processes. Accounting for this effect may be necessary when the permeability varies significantly over small distances in a heterogeneous medium.

[4] The macrodispersion resulting under such conditions has not been analyzed previously in the literature. It is the purpose of this paper to study this effect in 2-D, by considering both a small-fluctuation expansion and numerical simulation. First, we provide a small-fluctuation approach, by extending the well-known theory of *Gelhar and Axness* [1983]. Then, we present numerical results using an appropriate lattice Boltzmann simulation of tracer displacement based on the lattice BGK (Bhatnagar, Gross and Krook) model [Bhatnagar et al., 1954; Qian et al., 1992]. Here the Darcy viscous force is expressed as a body force. A lognormal hydraulic conductivity will be distributed to the lattice nodes which provide the mesoscopic scale, according to $\log(K) = \bar{f} + f'$, where f' is a gaussian perturbation. The macroscopic properties of the resulting porous medium will be measured at the scale of the lattice. It will be shown that theory and simulations agree well in the small fluctuation limit. As expected, the effect of the Brinkman correction is insignificant when the correlation length is not very small (for example, in typical field applications), in which case the classical results are obtained. In the opposite case, the macrodispersivity is found to decrease as the Brinkman effect becomes more important, reflecting the smoothing effect of the macroscale viscous effects on the velocity fluctuations.

[5] The paper is organized as follows: In section 2 we present an extension of the stochastic approach theory of *Gelhar and Axness* [1983] to the more general case of the Brinkman equation shown above. The flow simulation using the lattice BGK model is described in section 3. Theory and simulation are compared in section 4. The possible implications of the Brinkman correction on macrodispersion are discussed as a function of the correlation length.

2. Stochastic Analysis of Macrodispersion Using a Stokes-Darcy Equation

[6] We consider stationary viscous flow, described by the Stokes-Darcy (or Brinkman) equation

$$\vec{q} = -\frac{K}{\mu} \vec{\nabla} P + K \Delta \vec{q} \quad (2)$$

Here \vec{q} is the volume-averaged fluid velocity or specific discharge, K is the spatially varying permeability and P denotes pressure. In postulating (2) we made the widely-used assumption that $\mu_e = \mu$. In actuality, a rigorous derivation of the Brinkman correction has not appeared in the literature for arbitrary heterogeneity porous media. For example, *Dagan* [1979] derived a similar model but with the different coefficients

$$\vec{q} = -\frac{K}{\mu} \vec{\nabla} P + r^{(2)} \frac{K}{n} \Delta \vec{q} \quad (3)$$

where $r^{(2)} \approx 2.25 (1-n^2)/n^2$ for a certain case, and $r^{(2)}K/n \approx d^2/80$ for another. In (3), n is porosity, K the permeability

and d a typical pore size. In a more recent study, *Martin et al.* [2002] analyzed more rigorously the Brinkman term in a Hell-Shaw cell. They found, however that the averaged flow is well approximated by (3) with $r^{(2)}/n = 6/5$.

[7] In this paper, and without significant loss, we will use (3) with $r^{(2)}/n = r^{(2)} = 1$. Different values of the latter parameter can be readily incorporated in the final result, as will be shown below. As noted, the permeability will be lognormally distributed, as commonly done,

$$\log(K(\vec{r})) = f(\vec{r}) = \bar{f} + f'(\vec{r}) \quad , \quad \log K_I = \bar{f} \quad (4)$$

where f' is a perturbation of zero mean and variance σ_f^2 . As various spatial correlation laws give rather similar macroscopic behavior [*Hsu*, 1999, 2000], we choose an isotropic exponential covariance function with correlation length λ , hence

$$R_{ff}(\vec{\zeta}) = E(f'(\vec{r})f'(\vec{r} + \vec{\zeta})) = \sigma_f^2 \exp\left(-\frac{|\vec{\zeta}|}{\lambda}\right) \quad (5)$$

The transport of the tracer is described by the classical advection-dispersion equation,

$$\frac{\partial C}{\partial t} + \vec{q} \cdot \vec{\nabla} C = D_m \Delta C \quad (6)$$

with a local mesoscopic diffusion coefficient, D_m . In the above, we assumed isotropic mesoscale dispersion, leading to longitudinal and transverse dispersivities

$$\alpha_L = \alpha_T = \frac{D_m}{q} \quad (7)$$

where q is the mean flow velocity, the direction of which defines the x -axis (note that with this choice we have $\vec{q}_y = 0$). We also incorporated without loss of generality the porosity (assumed constant and uniform) into a rescaled time.

[8] For the small-fluctuation analysis, we will proceed following closely the approach of *Gelhar and Axness* [1983] and *Welty and Gelhar* [1991]. Small, random perturbations about the mean are assumed for the concentration, the specific discharge and the pressure: $C = \bar{C} + C'$, $q_\beta = \bar{q}_\beta + q'_\beta$ (where $\beta = x, y$) and $P = \bar{P} + P'$. The perturbation expansion is inserted in the advection-dispersion equation, the mass conservation equation and the Stokes-Darcy equation. To first-order in perturbations, we then obtain a set of equations, which are solved using the Fourier-Stieltjes representation. It is straightforward to show that the spectrum of the perturbations in velocity and concentration, $dZ_{q\beta}$ and dZ_C , are related to the spectrum of f' , dZ_f , as follows:

$$dZ_{q\beta}(\vec{k}) = K_I J_x \left(\frac{k^2 \delta_{\beta x} - k_\beta k_x}{k^2(1 + K_I k^2)} \right) dZ_f(\vec{k}) \quad (\beta = x, y) \quad (8)$$

where J_x is the mean hydraulic gradient which is in the x -direction (taking the mean value of (2) leads to $J_y = 0$), and

$$dZ_C = -\frac{1}{q(ik_x + k^2)} dZ_{q_x} \frac{\partial \bar{C}}{\partial x} \quad (9)$$

[9] It is evident that the effect of the Brinkman correction in (8) is the term $K_l k^2$ (the conventional Darcy result is recovered in the limit $K_l/\lambda^2 \rightarrow 0$). Note also that if $r^{(2)}/n \neq 1$, the coefficient K_l simply needs to be multiplied by $r^{(2)}/n$.

[10] Using the identity

$$\overline{a'b'} = \int_{-\infty}^{\infty} dZ_a^* dZ_b \quad (10)$$

we then obtain, after appropriate substitutions, the following expressions for the first-order velocity variances $\overline{q'_\beta q'_\beta}$:

$$\frac{\sigma_{q_x}^2}{q^2} = \frac{\overline{q_x^2}}{q^2} = \frac{3}{8} \frac{\sigma_f^2}{\gamma^2} \int_0^\infty \frac{udu}{(1+u^2)^{3/2} \left(1 + \frac{K_l}{\lambda^2} u^2\right)^2} \quad (11)$$

and

$$\frac{\overline{q'_y}}{\overline{q^2}} = \frac{1}{3} \frac{\overline{q'_x}}{\overline{q^2}} \quad (12)$$

Here we introduced $\gamma = K_{eff}/K_l$, the so-called flow factor [Gelhar and Axness, 1983], which to second-order in perturbations reads

$$\gamma = \frac{q}{K_l J_x} = 1 - \frac{\sigma_f^2 K_l}{4 \lambda^2} \int_0^\infty \frac{u^3 du}{\left(1 + \frac{K_l}{\lambda^2} u^2\right) (1+u^2)^{3/2}} \quad (13)$$

The classical result, $\gamma = 1$, for 2-D using Darcy's equation [Renard and de Marsily, 1997] is retrieved in the limit $K_l/\lambda^2 \rightarrow 0$.

[11] The mean dispersive flux, $\overline{q'_x c'}$, leads to the macrodispersivity. Taking into account the isotropic mesoscopic dispersivity, the longitudinal macrodispersivity, $\alpha = (D - D_m)/q$, where D is the macroscale dispersion coefficient, is

$$\alpha = \frac{\lambda^2 \sigma_f^2}{2\pi \gamma^2} \int_{-\infty}^{\infty} \frac{k_y^4 \alpha_L d\vec{k}}{(k_x^2 + \alpha_L^2 k^4) (1 + K_l k^2)^2 (1 + \lambda^2 k^2)^{3/2} k^2} \quad (14)$$

which in the limit of infinitely small mesoscopic dispersivity ($\alpha_L/\lambda = \alpha_f/\lambda \rightarrow 0$), reads

$$\alpha = \frac{\lambda \sigma_f^2}{\gamma^2} \int_0^\infty \frac{1}{\left(1 + \frac{K_l}{\lambda^2} u^2\right)^2 (1+u^2)^{3/2}} du \quad (15)$$

We need to point out that as $\sigma_{q_x}^2$ and α are calculated to first-order in perturbations, the term γ in (11) and (15) must also be replaced by its first-order expression, $\gamma = 1$, thus leading to the final results:

$$\frac{\sigma_{q_x}^2}{q^2} = \frac{\overline{q_x^2}}{q^2} = \frac{3}{8} \sigma_f^2 \int_0^\infty \frac{udu}{(1+u^2)^{3/2} \left(1 + \frac{K_l}{\lambda^2} u^2\right)^2} \quad (16)$$

and

$$\alpha = \lambda \sigma_f^2 \int_0^\infty \frac{1}{\left(1 + \frac{K_l}{\lambda^2} u^2\right)^2 (1+u^2)^{3/2}} du \quad (17)$$

Equations (16) and (17) are the final expressions for the variance of the velocity and the macrodispersivity, when the

flow field is generalized to also account for a macroscopic viscous (Brinkman) effect. In the limit where the correlation length is sufficiently large, the above reduces to the classical. In the more general case, the macrodispersivity can be expressed with the following functional dependence

$$\frac{\alpha}{\lambda} = g\left(\frac{K_l}{\lambda^2}\right) \sigma_f^2 \quad (18)$$

where in the small-fluctuation theory, the function $g\left(\frac{K_l}{\lambda^2}\right)$ is equal to the integral in (17). The above relation is in fact, general, and applies to arbitrary dimensions and without the limitation of the small fluctuation. Again, for a different Brinkman model, with $r^{(2)}/n \neq 1$, the terms containing K_l in the above expressions simply need to be multiplied by $r^{(2)}/n$.

[12] The above results will be compared to the numerical simulations described in the following section.

3. Lattice BGK Simulation of Flow and Displacement in a Porous Medium

[13] Since the pioneering work of Frisch *et al.* [1986], who demonstrated the ability of lattice gases to recover the full Navier-Stokes equations, an extended literature has become available [Rothman and Zaleski, 1997]. In the kinetic gas theory, simple collisions, preserving mass and momentum, give rise to gas transport properties, such as viscosity, mass and thermal diffusion. Statistical physics taking into account multiple collisions and interactions lead to a more elaborate description of the fluid state. By performing such statistical physics on a lattice with enough degrees of symmetry and freedom, the macroscopic behavior of the fluid is obtained.

[14] Following the classical lattice gas models, additional models have been developed. Here we will use one such version, namely the lattice BGK (Bhatnagar, Gross and Krook) model [Bhatnagar *et al.*, 1954], which uses population densities instead of particles, and contains the relaxation parameter ω_v at the collision step. The time evolution of the mass density, $N_i(\vec{r}, t)$, at the node \vec{r} and in the direction \vec{c}_i of the neighboring node $\vec{r} + \vec{c}_i$, is given by the relaxation equation

$$N_i(\vec{r} + \vec{c}_i, t + 1) = (1 - \omega_v) N_i(\vec{r}, t) + \omega_v N_i^{eq}(\vec{r}, t) \quad (\omega_v \in]0, 2[) \quad (19)$$

where N_i^{eq} is the equilibrium distribution [Qian *et al.*, 1992]. In the particular version of the model used in this work (the so-called D2Q9 model), the kinematic viscosity ν is related to the relaxation parameter using the relation

$$\nu = \frac{1}{3} \left(\frac{1}{\omega_v} - \frac{1}{2} \right) \quad (20)$$

Although, strictly speaking, developed to simulate flow of a homogeneous fluid, lattice gas models can readily be adapted to account for flow in a porous medium by introducing the Darcy viscous force as an external force [Spaid and Phelan, 1997; Martin *et al.*, 2002]. This inno-

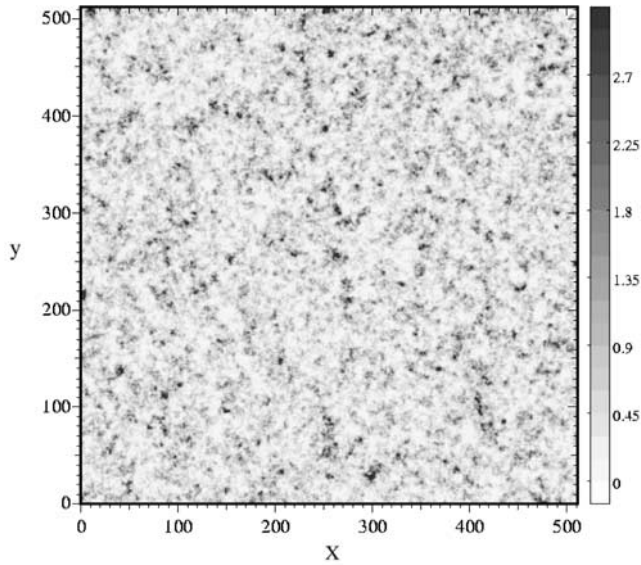


Figure 1. Gray-level map of the permeability field of one realization of a porous medium, characterized by a lognormal isotropic distribution of mean $\bar{f} = -1$, root-mean square (RMS) $\sigma_f = 0.8$ and correlation length $\lambda = 3.4$ in lattice units.

vative method to account for porous media effects, leads to the Navier-Stokes-Darcy (NSD) equation

$$\frac{\partial \vec{V}}{\partial t} + (\vec{v} \cdot \vec{\nabla}) \vec{V} = -\frac{\vec{\nabla} P}{\rho} - \frac{\nu}{K} \vec{V} + \nu \Delta \vec{V} \quad (21)$$

While it does not necessarily rigorously describe the flow in a porous medium at arbitrary Reynolds numbers, this equation does lead to the widely used Brinkman correction at conditions of a stationary state and at low Reynolds numbers,

$$\vec{\nabla} P = -\frac{\mu}{K} \vec{V} + \mu \Delta \vec{V} \quad (22)$$

The macroscale viscous effect (the Laplacian $\Delta \vec{V}$) allows to smooth velocity discontinuities associated with Darcy's law in places of permeability changes. In the general form of the Brinkman equation (1), the relative weight of the two friction terms may be tuned with the help of μ_e . In our case, where $\mu_e = \mu$, this may be done by adjusting the value of the ratio K/l^2 , where l is the characteristic length of the velocity variations (i.e. the correlation length, λ , of the stochastic distribution).

[15] Mesoscopic diffusion is implemented in such a way that the advection-dispersion equation for the tracer concentration, $C(\vec{r}, t)$, is recovered from the relaxation equation of the lattice values of $C_i(\vec{r}, t)$ with a relaxation parameter ω_D [Flekkøy, 1993; Rakotomalala et al., 1997]. We then obtain the conventional advection-dispersion equation, where the mesoscopic diffusion coefficient, D_m , is related to ω_D by

$$D_m = \frac{1}{3} \left(\frac{1}{\omega_D} - \frac{1}{2} \right) \quad (23)$$

In the lattice BGK simulations, the typical size of the lattice was 256×512 , with 256 nodes in the x -direction. Quantitative measurements may be obtained from the simulations, using as time and length scales the time step and the lattice mesh, respectively. The velocity is therefore in units of lattice mesh per time step.

[16] The permeability field was generated by convolving a white noise with an ad-hoc correlation function, namely

$$h(x, y) = \exp \left[-\left(\frac{x^2}{\delta^2} + \frac{y^2}{\delta^2} \right)^{1/3} \right] \quad (24)$$

where δ is a parameter ranging in the interval $[0.1, 0.9]$. This function provides a nearly exponential correlation function in the range of correlation lengths used. Figure 1 shows a typical permeability field. The corresponding measured covariance function is shown in Figure 2. By best-fitting the covariance function in a semi-log plot using a straight line with slope $-1/\lambda$, as dictated by (5), the value of λ can be obtained. The solid line in Figure 2 is the resulting exponential. In the analysis we took $\vec{V} = \vec{q}$. The computational method has the advantage of being very fast (5 s CPU time for a mesh of size 256×512). The resulting computational savings enable us to use a different porous medium for each simulation point.

4. Results and Discussion

[17] The first results obtained from the simulations pertain to the effective permeability, K_{eff} , as a function of the porous medium characteristics. This effective permeability was obtained by postulating a macroscopic Darcy law across the two boundaries of the porous medium, and using the relationship between the mean flow rate and pressure drop between the two boundaries. In the simulations, we varied the exponential of the log permeability, K_l , in the range $[0, 20]$, the RMS, σ_f , in the range $[0, 1.5]$ and the correlation length, λ , in the range $[1, 4]$.

[18] It was found that the flow factor, $\gamma = K_{eff}/K_l$, obeys the prediction given by (13), over the range of parameters used. This is illustrated in Figure 3, which displays the simulation values for γ (as dots) versus σ_f , while keeping K_l/λ^2 constant, equal to 0.09 (circles) and 1 (squares),

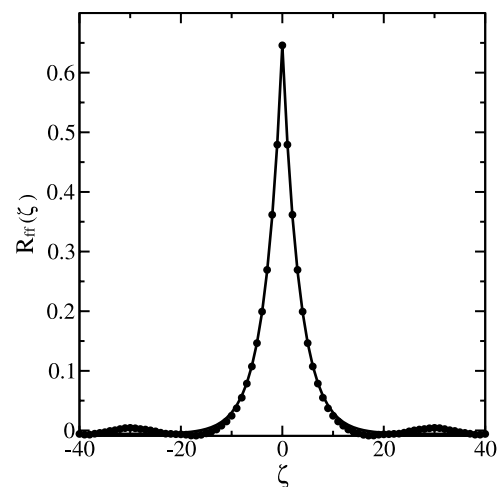


Figure 2. Measured covariance function (dots) of the lognormal isotropic distribution in Figure 1. The value of λ was obtained by an exponential fit (line) using equation (5).

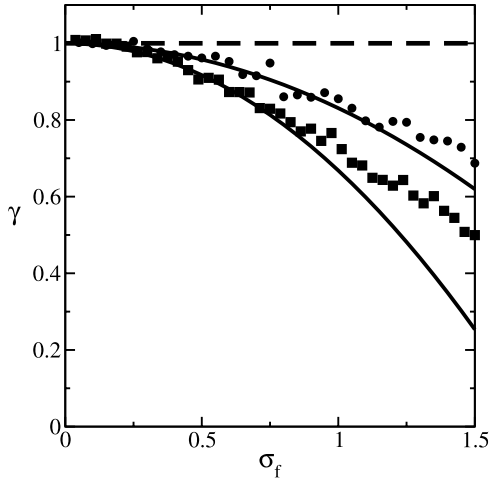


Figure 3. Flow factor, γ , i.e., the ratio of the simulated permeability, K_{eff} , to the exponential of the mean log hydraulic permeability, $K_l = \exp(\bar{f})$, versus the RMS, σ_f , for $K_l/\lambda^2 = 0.09$ (circles) and 1 (squares). The lines through the data are given by the theoretical equation (13). The dashed line corresponds to the Darcy's law regime, $K_l/\lambda^2 \rightarrow 0$.

respectively. The simulated flow factor is in good agreement with the theory (solid lines), not only at low values of σ_f which is as expected, but also at larger values. Parameter γ decreases with σ_f , the decrease being less pronounced when the Darcy regime ($K_l/\lambda^2 \rightarrow 0$, dashed line) is approached.

[19] Subsequently, we considered the spreading of a tracer in the disordered velocity field resulting from the heterogeneity of the porous medium. The macroscopic dispersion coefficient, D , was determined at different distances from the inlet, as a function of time [de Arcangelis *et al.*, 1986]. The dispersivity, $\alpha = (D - D_m)/q$, is the quantity of interest for tracer dispersion. In the present simulations, the local mesoscopic dispersivity is isotropic, $\alpha_L = \alpha_T = D_m/q = 0.025$.

[20] Figure 4 displays the dispersivity, α , normalized by the correlation length, λ , as a function of the distance from

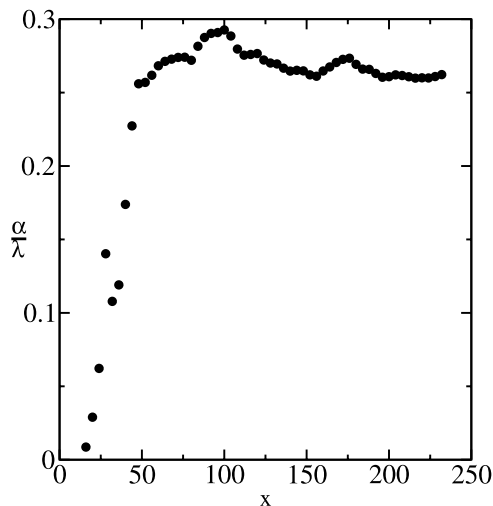


Figure 4. Normalized macrodispersivity, α/λ , versus the distance, x , from injection, for $q = 0.004$, $\bar{f} = -1$, $\sigma_f = 0.4$ and $\lambda = 2$.

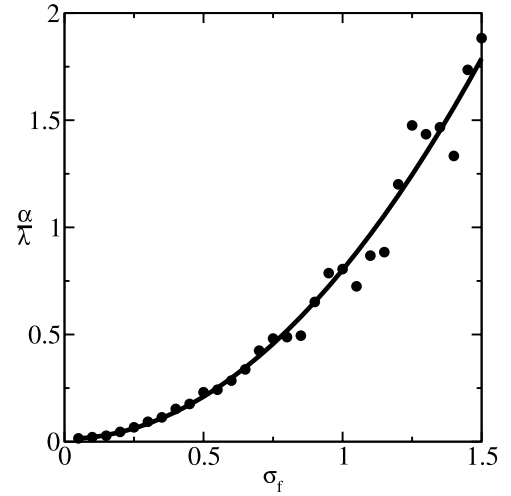


Figure 5. Normalized macrodispersivity, α/λ , versus the RMS, σ_f , for $K_l/\lambda^2 = 0.09$. The solid line is a quadratic fit to the data, $\frac{\alpha}{\lambda} = 0.8 \sigma_f^2$.

the inlet: As expected, the macrodispersivity increases with distance, until the tracer samples the heterogeneity field. The coefficient eventually stabilizes to an asymptotic value, provided that the sample is large enough. In the simulations, this asymptotic behavior is obtained after a distance approximately greater than 120 nodes (which is about half of the length of the samples used).

[21] To test the prediction on the behavior of α , given by (18), we varied σ_f and/or the ratio K_l/λ^2 . Figure 5 shows a plot of the dispersivity, α , normalized by the correlation length, λ , versus the RMS, σ_f , for $K_l/\lambda^2 = 0.09$. Figure 5 shows that a quadratic law fits reasonably well our data over the range of variances used. The line through the data is given by $\alpha/\lambda = 0.8 \sigma_f^2$ where the factor 0.8 is close to the value $g(0.09) = 0.84$.

[22] The effect of the parameter K_l/λ^2 , which measures the importance of the Brinkman correction, was investigated, next. Figure 6 shows a plot of the ratio of the

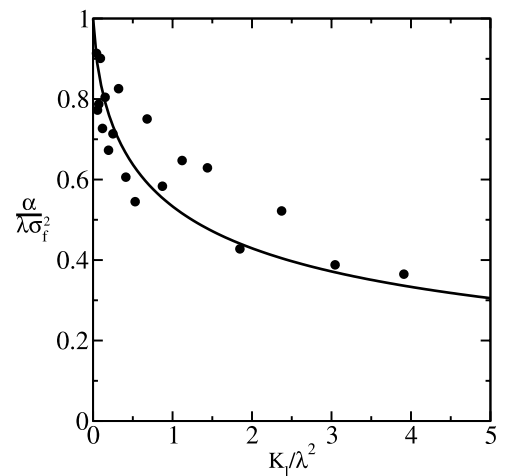


Figure 6. Ratio of the normalized macrodispersivity to the variance, $\alpha/\lambda\sigma_f^2$, versus the normalized permeability, K_l/λ^2 , for $\sigma_f = 0.8$. The line through the data is the theoretical result (17).

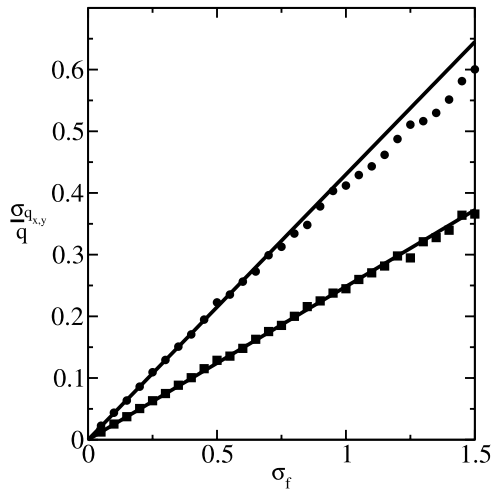


Figure 7. Normalized RMS, σ_{q_x} and σ_{q_y} , of the velocity fluctuations in the directions parallel (circles) and transverse (squares) to the mean flow direction, versus σ_f . The lines through the data correspond to the theoretical first-order in σ_f approximation of the stochastic theory ((12) and (16)).

normalized dispersivity, α/λ , to the variance, σ_f^2 versus K_l/λ^2 . For small values of K_l/λ^2 , we approach the classical Darcy limit $\alpha/\lambda \sigma_f^2 \sim 1$. Given that typical field values are of the order of 10^{-4} or smaller, the importance of the Brinkman correction to field dispersivities should be negligible, therefore. The correction becomes important as K_l/λ^2 increases, requiring very small correlation lengths, which are possible in laboratory applications. The plot shows that the dispersivity decreases with increasing values of K_l/λ^2 , namely inclusion of the Brinkman effect leads to smaller spreading. We physically interpret this trend by noting that the Brinkman correction leads to smoother velocity fields, hence to a decrease of the velocity variance and macrodispersion. The results of Figure 6 should not be extrapolated too liberally. When the ratio K_l/λ^2 becomes larger than an $O(1)$ value, it is questionable that the problem can be described by the continuum formalism we used above. In the range where this continuum formalism is expected to be valid, the macrodispersivity does not become smaller than about half of its classical value. Thus, in practical terms, the Brinkman correction is expected to have a negligible effect for field conditions and an effect of less than a factor of two when the effect is most pronounced (very small correlation lengths). Figure 6 also shows the comparison of the simulations with the theoretical result

$$g\left(\frac{K_l}{\lambda^2}\right) = \int_0^\infty \frac{1}{\left(1 + \frac{K_l}{\lambda^2} u^2\right)^2 (1 + u^2)^{3/2}} du \quad (25)$$

The two are found in good agreement. Equation (15) seems to be valid for a range of values of σ_f greater than expected, provided that we take $\gamma = 1$. We find analogous results for (11): Figure 7 displays the velocity fluctuations, σ_{q_x} and σ_{q_y} , normalized by the mean flow velocity, q , versus the RMS, σ_f . We note that σ_{q_x} increases linearly with σ_f in a large range of σ_f values. Thus, provided that $\gamma = 1$, (11) seems to be valid over a large range of values of the perturbation. This result is

consistent with Chin ([Chin, 1997]), who found that Gelhar's calculations are robust for large σ_f provided that $\gamma = 1$. We conclude that the theory at the first-order approximation in perturbations is more robust than expected.

[23] For completeness, Figure 8 shows the velocity distribution (dots) in the mean flow direction, for a mean velocity $q = 0.004$ and a variance $\sigma_{q_x}^2 = 0.36 q^2$. The shape of the distribution is not very different from a lognormal (line). Lognormal velocity distributions were measured experimentally by Lebon *et al.* [1996] in a glass-bead pack. Therefore one may think of heterogeneous porous media simulations, as good candidates to model dispersion phenomena in glass-bead packs, which are often considered as the paradigm of homogeneous model porous media.

5. Conclusions

[24] We studied macrodispersion in porous media by extending Darcy's law to also account for the Brinkman correction. The latter is necessary when permeability changes fast at a relatively small scale, and in general is a more complete description of the underlying flow. A small-fluctuation expansion was derived. The theoretical results were then compared to numerical simulations using a lattice BGK method, which proved to be quite efficient for that application. Using an isotropic exponentially decaying correlation function, we calculated the effective permeability, the variance of the longitudinal and transverse velocity fluctuations, and the tracer dispersivity as a function of parameters, including the correlation length, λ , and the mean, K_l , and variance, σ_f^2 , of the lognormal permeability field. The results contain the additional parameter K_l/λ^2 , the sensitivity to which was studied. When the latter takes small values, the classical results were obtained. Field conditions are under this limit, hence the Brinkman effect on the field macrodispersivity is negligible. As the value of K_l/λ^2 increases (for example, for small correlation lengths), the macrodispersivity decreases reflecting the smoothing effect of the Brinkman correction on the velocity field. For practical values of the parameters, this reduction in macrodispersivity would be no larger than 50% of the classical expression. The small fluctuation theory was compared to the simulations and found to be quite accurate, provided that

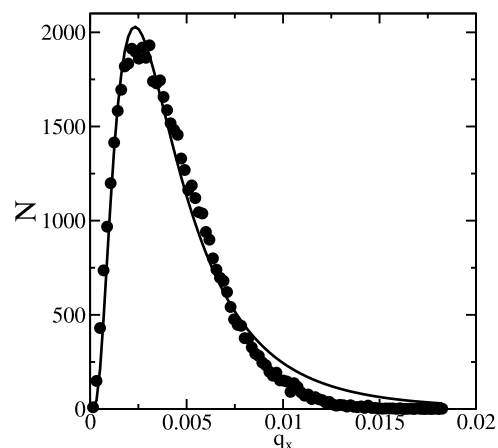


Figure 8. Distribution of the x component of the velocity, for a mean velocity $q = 0.004$ and a variance $\sigma_{q_x}^2 = 0.36 q^2$ (dots). The lognormal function (line) is a guide to the eye.

it was consistently applied (namely by not mixing first-order with second-order expansions).

[25] **Acknowledgments.** We acknowledge stimulating discussions with Professors F. Delay and J.-P. Hulin. This work was partly supported by IDRIS (project 014052) and the French National Program of Research in Hydrology (PNRH). All these sources of support are gratefully acknowledged.

References

- Ababou, R., D. McLaughlin, L. W. Gelhar, and A. F. B. Tompson, Of macrodispersion in aquifers, *Transp. Porous Media*, 4, 549–565, 1989.
- Bellin, A., P. Salandin, and A. Rinaldo, Simulation of dispersion in heterogeneous porous formations: Statistics, first-order theories, convergence of computations, *Water Resour. Res.*, 28, 2211–2227, 1992.
- Bhatnagar, P. L., E. P. Gross, and M. Krook, A model for collision processes in gases, I, Small amplitude processes in charged and neutral one-component systems, *Phys. Rev.*, 94, 511–525, 1954.
- Brinkman, H. C., A calculation of the viscous exerted by a flowing fluid on a dense swarm of particles, *Appl. Sci. Res., Sect. A*, 1, 27–39, 1947.
- Chin, D. A., An assessment of first-order stochastic dispersion theories in porous media, *J. Hydrol.*, 199, 53–73, 1997.
- Dagan, G., The generalization of Darcy's law for non-uniform flows, *Water Resour. Res.*, 15, 1–7, 1979.
- Dagan, G., Stochastic modeling of groundwater flow by unconditional and conditional probabilities: 2. The solute transport, *Water Resour. Res.*, 18, 835–848, 1982.
- Dagan, G., Solute transport, in heterogeneous porous formation, *J. Fluid Mech.*, 145, 151–177, 1984.
- Dagan, G., *Flow and Transport in Porous Formations*. Springer-Verlag, New York, 1989.
- de Arcangelis, L., J. Koplik, S. Redner, and D. Wilkinson, Hydrodynamic dispersion in network models of porous media, *Phys. Rev. Lett.*, 57, 986–999, 1986.
- Flekkøy, E. G., Lattice BGK model for miscible fluids, *Phys. Rev. E.*, 47, 4247–4271, 1993.
- Frisch, U., B. Hasslacher, and Y. Pomeau, Lattice-gas automata for the Navier-Stokes equation, *Phys. Rev. Lett.*, 56, 1505–1508, 1986.
- Gelhar, L. W., and C. L. Axness, Three-dimensional stochastic analysis of macrodispersion in aquifers, *Water Resour. Res.*, 19, 161–180, 1983.
- Hsu, K. C., A general method for obtaining analytical expressions for the first-order velocity covariance in heterogeneous porous media, *Water Resour. Res.*, 35, 2273–2277, 1999.
- Hsu, K. C., General first-order expressions for solute transport in two- and three-dimensional randomly heterogeneous porous media, in *Theory, Modeling, and Field Investigation in Hydrogeology: A Special Volume in Honor of Shlomo P. Neuman's 60th Birthday*, edited by D. Zhang and C. L. Winter, *Spec. Pap. Geophys. Soc. Am.*, 348, 91–104, Boulder, Colo., 2000.
- Jussel, P., F. Stauffer, and T. Dracos, Transport modeling in heterogeneous aquifers: 2. Three-dimensional transport model and stochastic numerical tracer experiments, *Water Resour. Res.*, 30, 1819–1831, 1994.
- Lebon, L., L. Oger, J. Leblond, J.-P. Hulin, N. S. Martys, and L. M. Schwartz, Pulsed gradient NMR measurements and numerical simulations of flow velocity distribution in spheres packing, *Phys. Fluids*, 8, 293–301, 1996.
- Martin, J., N. Rakotomalala, and D. Salin, Gravitational instability of miscible fluids in a Hele-Shaw cell, *Phys. Fluids*, 14, 902–905, 2002.
- Qian, Y. H., D. d'Humières, and P. Lallemand, Lattice BGK models for Navier-Stokes equation, *Europhys. Lett.*, 17, 479–484, 1992.
- Rakotomalala, N., D. Salin, and P. Watzky, Miscible displacement between two parallel plates: BGK lattice gas simulations, *J. Fluid Mech.*, 338, 277–297, 1997.
- Renard, P., and G. de Marsily, Calculating equivalent permeability: A review, *Adv. Water Resour.*, 20, 253–278, 1997.
- Rothman, D. H., and S. Zaleski, *Lattice-Gas Cellular Automata*, Cambridge Univ. Press, 1997.
- Rubin, Y., Stochastic modeling of macrodispersion in heterogeneous porous media, *Water Resour. Res.*, 26, 133–141, 1990.
- Spaid, M. A. A., and F. R. Phelan Jr., Lattice Boltzmann methods for modeling microscale flow in fibrous porous media, *Phys. Fluids*, 9(9), 2468–2474, 1997.
- Tompson, A. F. B., and L. W. Gelhar, Numerical simulation of solute transport in three-dimensional, randomly heterogeneous porous media, *Water Resour. Res.*, 26, 2541–2562, 1990.
- Welty, C., and L. W. Gelhar, Stochastic analysis of the effects of fluid density and viscosity variability on macrodispersion in heterogeneous porous media, *Water Resour. Res.*, 27, 2061–2075, 1991.

J. Martin, N. Rakotomalala, D. Salin, and L. Talon, Laboratoire FAST, Campus Universitaire, Bâtiment 502, 91405 Orsay Cedex, France. (talon@fast.u-psud.fr)

Y. C. Yortsos, Department of Chemical Engineering, University of Southern California, Los Angeles, CA 90089-1211, USA.